Visualization study on premature CHF during two phase flow instability in narrow, vertical, rectangular channel

HE Haisha, CAO Xiaxin[1], HU Jian, LI Na, and YANG Peixun

1. College of Nuclear Science and Technology, Harbin Engineering University, Harbin, 150000, China (caoxiaxin@hrbeu.edu.cn)

Abstract: As one of the three major criteria for reactor design, the prediction of critical heat flux (CHF) is of great concern. Traditionally, CHF can be roughly divided into departure from nucleate boiling (DNB) and dryout according to exit equilibrium quality (x_e). DNB mostly happens when x_e<0, while dryout occurs when x_e>0. Recently, however, another type of CHF, which is called premature CHF (PM-CHF), is observed during two-phase flow instability through high-speed photography. Although premature CHF is not as high as stable CHF, it can cause an abrupt rise of heating wall temperature, which may do much damage to heater. Plate type fuel assemmbly is widely used in research reactors and integration reactors because of its large cooling area and compactness. But few study focused on premature CHF in narrow rectangular channel. Therefore, visualization study on premature CHF during two phase flow instability for upward vertical flow in narrow rectangular channel heated from one side was experimentally performed. The flow channel is 700 **mm** long, 70 **mm** wide and 2.7 **mm** in gap. The coolant is deionized water. The premature CHF was achieved by rising heating power step by step in low inlet subcooling(15~34 **K**), low mass flux (117~337 **kg/(m^2•s)**) and high heat flux (~177 **kW/m^2**) under atmospheric pressure. Results showed that in the process of gradually increasing the heating power, small bubbles, bubble growth, bubble coalescence and intermittent flow can be successively observed at the channel outlet. During the intermittent flow, the fluid and vapor alternately passed through the channel. With the increase of heating power, the intermittent oscillation period got longer and longer and the amplitude of heating plate temperature got larger and larger. Eventually, the system got to the state of premature CHF. Besides, before the occurrence of premature CHF there existed the fluctuation of pressure drop and flow rate. Therefore, it is reasonable to monitor the fluctuation of pressure drop and flow rate to prevent premature CHF. A boundary map to prevent premature CHF is depicted in terms of dimensionless inlet subcooling number and dimensionless phase change number based on the present experimental configuration.

Keyword: premature CHF; visualization; narrow; rectangular channel

1 Introduction

For a long time, plate type fuel assemmbly with narrow rectangular channel structure has been widely used in research reactors and integration reactors. CHF is one of the most important criteria in reactor design, which is related to the reactor power output effectiveness and safety of operation under accident condition. Lots of efforts has been devoted to clarifying the the mechanism of DNB and dryout in narrow rectangular channel to provide a proper prediction of CHF. But recently another type of CHF named after premature CHF (PM-CHF) was observed in the research of two-phase flow instability in microchannels [1]. Although premature CHF is not as high as stable CHF, it can cause an abrupt rise of heating wall temperature, which may do much damage to heater. Therefore, it is essential to establish a profound understanding of this new type of CHF.

The majority of study on PM-CHF was based on microchannels because of the astonishing prosperity of microelectromechanical system. Qu and Mudawar [2][3] performed a series of experiments in a water-cooled two-phase micro-channel heat sink containing multiple micro-channels. When promoting heat flux to CHF, they observed flow instabilities induced vapor backflow into the heat sink's upstream plenum, which resulted in CHF. And the magnitude of this kind of CHF is virtually independent of inlet temperature but increases with increasing mass velocity. In addition, the CHF can not be well predicted by previous correlations that are quite accurate at predicting CHF in single mini-channels. Bergles and Kandlikar [1] reviewed several previous CHF studies and concluded that the PM-CHF is the result of an upstream compressible volume instability or the parallel channel Ledinegg instability.

Received date: November 14, 2018
(Revised date: January 12, 2019)

Kandlikar and Steinke [4] utilize high-speed photography to study the flow pattern of boiling in parallel mini-channels and they observed reversed flow and vapor flow back into the inlet mainfold. Lee Kim and Mudawar [5][6] attributed this phenomenon of vapor backflow to the weak momentum of incoming liquid and small inlet subcooling. Lee *et al.*[7] conducted an experiment to explore the characteristics of premature and stable CHF in narrow rectangular channel. With the increase of the heating power, there would be an irremovable pressure drop fluctuation, to which the authors attributed the periodic back flow. Premature CHF generally occurs in a subcooled boiling regime (x_e < 0) while stable CHF occurs over the saturated liquid condition (x_e > 0). The premature CHF could be eliminated by an additional pressure drop over 0.4 bar by an throttling valve in the upstream of the channel inlet. Kaya *et al.*[8] found that Fast Fourier Transform (FFT) could be used as a detection tool for premature CHF. Because side lobe energy obtained from FFT profiles becomes significantly higher at the inception of premature CHF.

As seen from the above literature review, most researches on PM-CHF were carried out in microchannel with the equivalent diameter less than 1 **mm**. There are few studies on PM-CHF in narrow rectangular channel. The present study aims at explore the mechanism of PM-CHF of flow boiling in vertical narrow rectangular channel.

2 Experiment method

The apparatus of this experiment is shown in Fig.1. The experiment apparatus consisted of main loop and the secondary loop. The secondary loop provided heat sink for the main loop. The main loop was composed of a rectangular test section, a condenser, a centrifugal pump, a pressurizer and a preheater. The heated water is cooled by the condenser, which transport the heat to the final heat sink—atmosphere through secondary loop. The pump and the preheater are used to maintain flow rate and system pressure constant respectively. The inlet temperature of the test section is adjusted by the PID regulating circuit in the electric cabinet. The Y-type filter installed at the entrance of the experimental section is used to filter out impurities in the water to prevent clogging. The volume flow rate is measured by electromagnetic flowmeter equipped near the entrance of the preheater. And two N-type thermocouples are installed in the inlet and outlet of the test section to measure the inlet and outlet liquid temperature respectively.

As shown in Fig.3, the test section consists of quartz glass visible window, electric heating plate, o type sealing ring. The quartz glass and electric heating plate assemble the narrow rectangular channel, which is 670 **mm** long with a width-gap ratio of 26. The electric heating plate is 3 mm thick, and is electrically insulted from other connected parts by means of special method. Through the hole on the lower bearing structure, armored thermocouples are welded onto the outer-wall of the heating plate to measure the outer-wall temperature.

Figure 2 shows the power control and data acquisition system. In the middle of the heating plate distributed 11 thermocouples in a column with equal distance of 50 **mm**. There are another four detection thermocouples on the right side of the heating plate, which are connected to a PLC. The PLC reads the temperature data every 10 **ms** and subtracts it from the previous data to get a difference. Either the temperature or the the temperature difference exceed a set value, the PLC sends a message to relay to cut off power supply.

Before experiment, the preheater and the heating plate of the test section was turned on to heat the water to near saturation for half an hour to expel non-condensable gases. During formal experiment, the flow rate was adjusted to a set value by adjusting the valve at the exit of the pump. And the inlet temperature of the test section was maintained to the set value by the PID regulating circuit. Subsequently, the heating power of heating plate was gradually increased in a certain step until CHF is reached. In the meantime, the measured parameters, including volume flow rate, pressure drop over the test section and temperature of heating plate and liquid, was recorded by the Labview software. The experimental parameters' range are shown as Table 1.

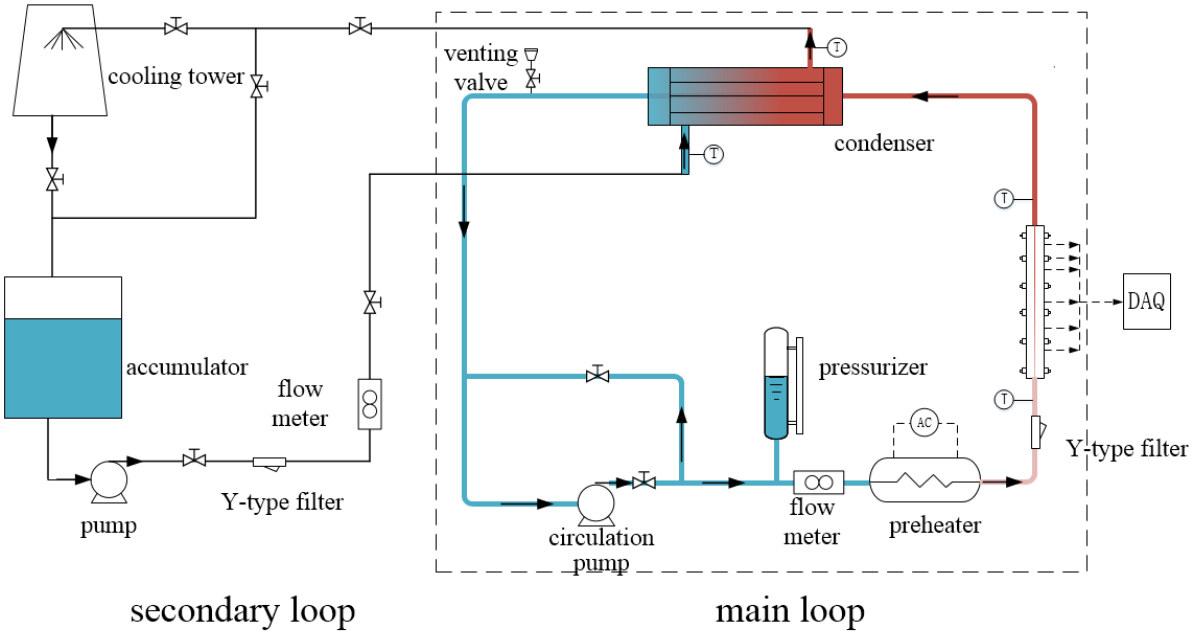

Fig.1 Experiment loop.

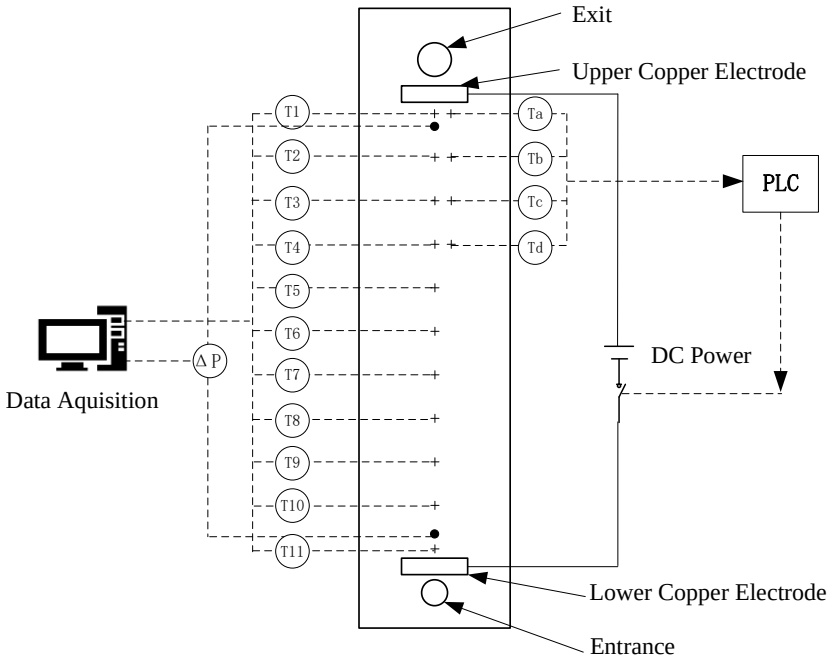

Fig.2 Power control and data acquisition.

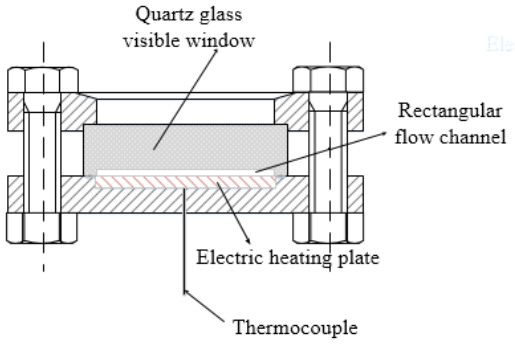

Fig.3 Test section.

Table. 1 Experimental parameters and ranges.

Parameters	Range
System pressure (MPa)	0.141
Heat flux (kW/m^2)	0–177
Mass flux [kg/(m^2 s)]	117–337
Inlet water subcooling（℃）	15, 20, 34

3. Results and discussion

3.1 Visualization of two-phase flow pattern

To investigate the relevance of PM-CHF and the flow structure, high-speed photography was used to record the images in narrow rectangular channel heated from one side over the process of elevating heating power.

The operating condition of q=83 **kW/m²**, G=205 **kg/(m²•s)**, P=0.141 **MPa**, and ΔT_{in}=15**℃** was chose to illustrate the problem. In the process of elevating heating power, the flow pattern was always stable bubbly flow when heat flux was relatively low. When heat flux reached 83 **kW/m²**, the reversed flow happened. Fig.4 recorded the process. At 119.4 **s**, coalesced bubbles was observed around the right corner near the exit because the corner of the heating plate was cooled not as sufficiently as the middle. At 120.7 **s**, the coalesced bubble appeared at the middle of the channel and grew larger and larger and eventually disappeared at the exit. Velocity of coalesced bubble was estimated to be 0.44 **m/s**. At 122.9 **s**, the vaporization intensified so the coalesced bubbles began to merge into vapor clots. The formation of vapor clot would cause local high pressure because the large difference of density of vapor and water. Therefore, as the photo from 122.9 **s** to 125 **s** shows, the negative pressure drop over the test section forced the liquid retreat to the channel entrance. Immediately, however, the driving pressure provided by the pump forced the vapor out of channel. Photos from 125 **s** to 132.2 **s** shows the process of liquid rewetting the heating plate.

From the above discussion it is concluded that the reversed flow could be divided into three stages: bubble coalescence, liquid retreat and rewetting. The stage of bubble coalescence is from the first appearance of coalesced bubble to the appearance of vapor clot. The stage of liquid retreat is from the appearance of vapor clot to the moment at which the liquid retreated to the channel entrance. The stage of rewetting is from the moment at which the liquid retreated to the channel entrance to the moment at which the heating plate was completely covered by liquid. The rewetting stage occupied more than 50% of the period.

Fig.5 shows the trend of outer wall temperature and volume flow rate during one reversed flow period. Before the bubble coalescence, the volume flow rate had already in the process of decline. The decline of flow rate weakened the convective heat transfer so the vaporization was intensified to promote the formation of vapor clot. After the formation of vapor clot, the flow rate decreased to a minimum value. In the meantime, the outer wall temperature increased to its highest value. Subsequently, the flow rate gradually increased to a steady state. In the meantime, the outer wall temperature decreased. Due to the heat capacity of the heating plate, the outer wall temperature decreased for a while after the period.

When heat flux was increased to a higher level, reversed flow could be divided into four stages rather than three stages.

The new stage observed was the choking between the liquid retreat and rewetting. Fig.6 shows the flow pattern under 99 **kW/m²**. Different from the condition in relatively low heating flux, the flow under 99 kW/m² would be stagnant for quite a long time after the liquid retreated to the channel entrance. As Fig.6 shows, after the flow retreat at 438.5 **s**, the liquid attempted several times to flow back to the exit. But the heating flux was so high that once the liquid attempted to rewet the heating plate the liquid would vigorously vaporize immediately. Due to rewetting obstruction, the temperature of heating plate would increase rapidly. When the pressure of the vapor decreased due to the condensation of the condensater, the liquid returned and rewetted the heating plate.

Fig.7 shows the trend of outer wall temperature and volume flow rate during one reversed flow period under the heat flux of 99 **kW/m²**. The outer wall temperature and volume flow rate under 99 **kW/m²** showed the same trend as that under 83 **kW/m²**. But there were still some differences. First, the magnitude of reversed flow period under high heat flux was larger than that under lower heat flux. The period under 83 **kW/m²** was 12.8 **s** while the period under

99 **kW/m²** was 39 **s**. Secondly, in the stage of choking existed fast flow rate fluctuation with 13 times in 33 **s**, while the flow rate recovered to normal value right away after reaching the minimum value. Finally, the amplitude of outer wall temperature fluctuation under 99 **kW/m²** was higher than that under 83 **kW/m²**. Because when heat flux was 99 **kW/m²** there existed choking stage, during which the heating plate could not be rewetted completely by liquid.

From the above comparing, it can be found that not only a new stage appeared in the cycle but also the time from flow excursion to restabilization got longer. To investigate the relevance between the period and the PM-CHF, a figure of T varying with q was depicted. T is defined as the time from the formation of vapor clot to the completion of rewetting. As the Fig.11 shows, when the heat flux was below 68 **kW/m²**, the flow was stable. So the period was 0 **s**. As the heat flux increased, the reversed flow appeared and the period was small (about 10 **s**). With further increase of the heat flux, the period got longer and longer. When period reached its maximum (about 60 **s**), the PM-CHF was triggered. It is reasonable to assume that long period prevents the cooling of heating plate and results in the appearance of PM-CHF.

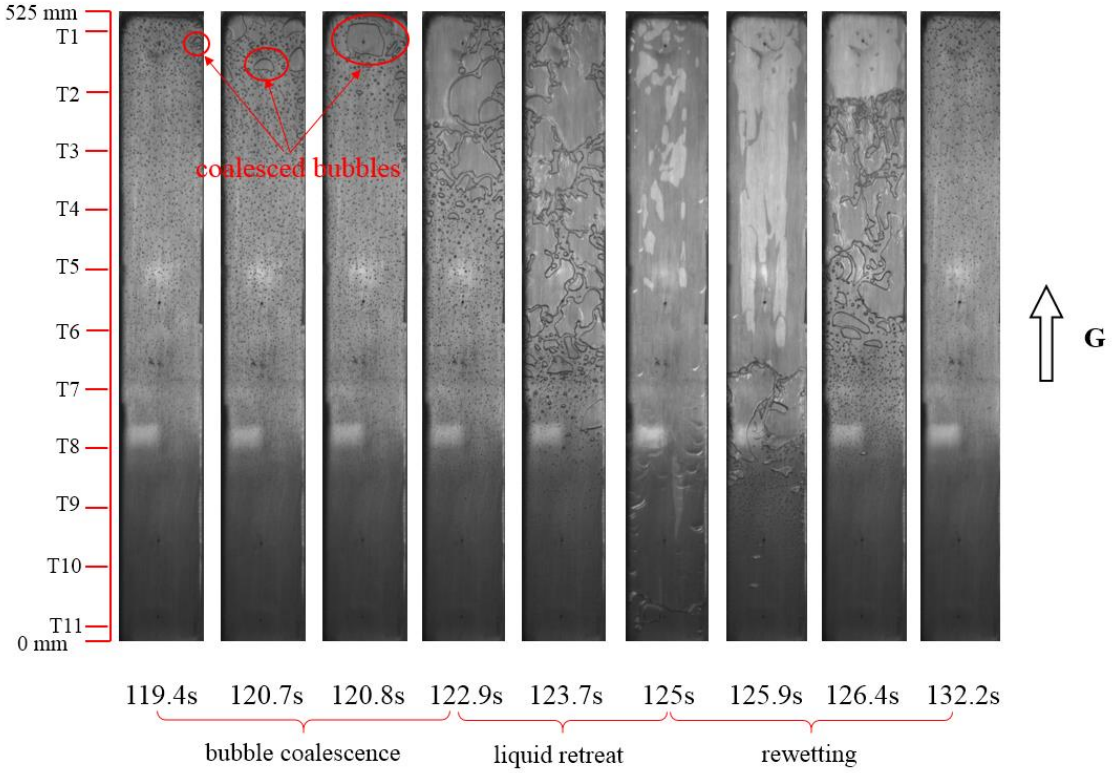

Fig.4 Flow pattern during reversed flow for q=83 kW/m², G=205 kg/(m²•s), P=0.141 MPa, and ΔT_{in}=15℃.

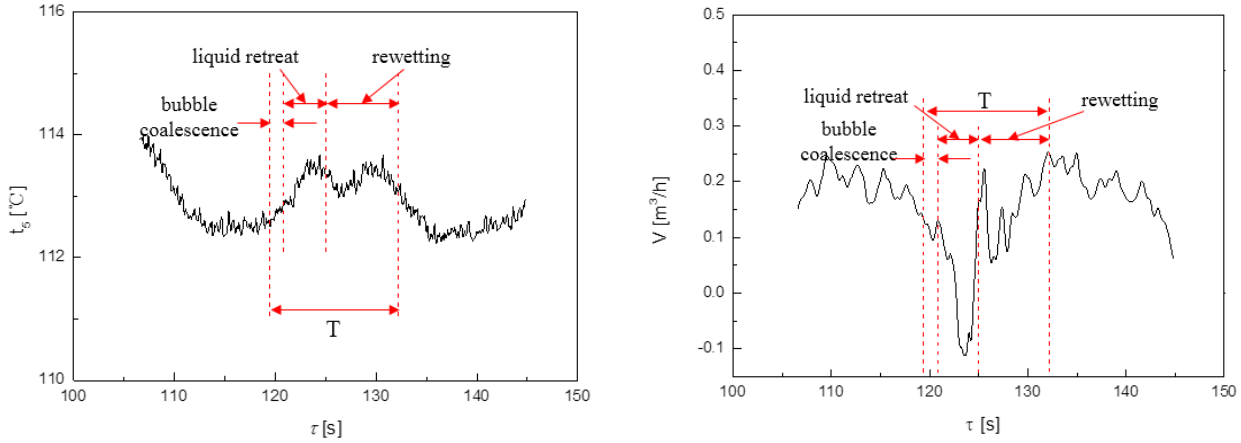

(a) Outer wall temperature. (b) Volume flow rate.

Fig.5 parameters' fluctuation during one reversed flow period, *q*=83 kW/m², *G*=205 kg/(m²•s), *P*=0.141 MPa, and ΔT_{in}=15℃.

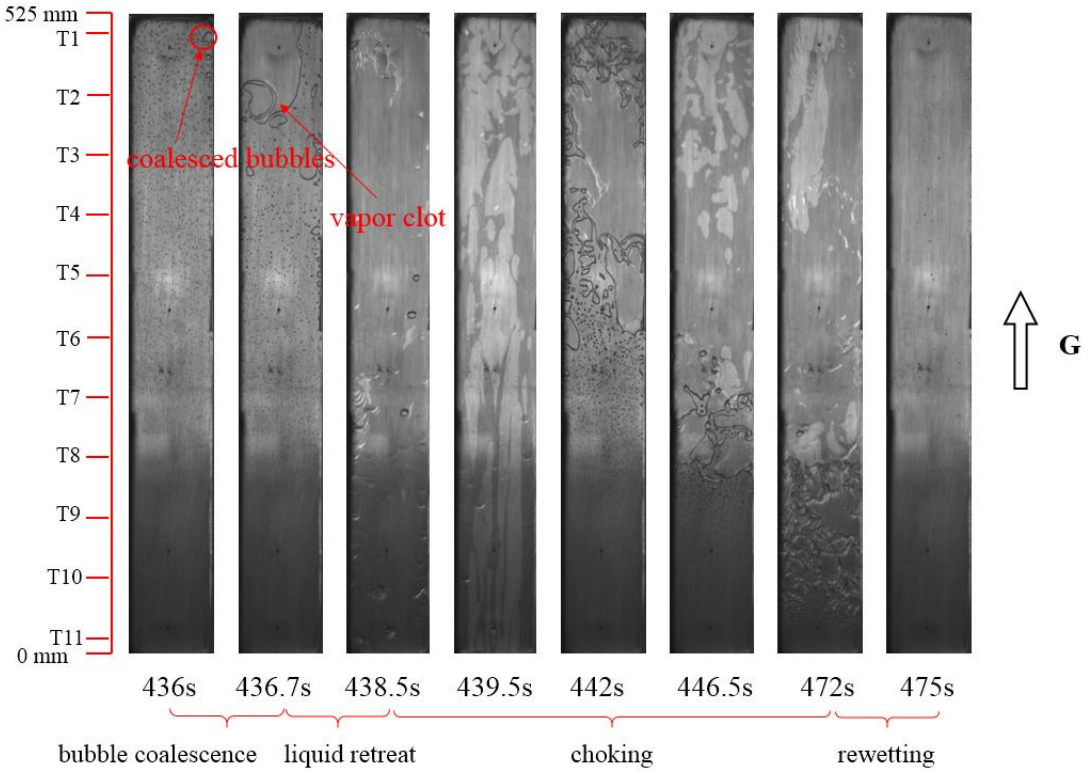

Fig.6 Flow pattern during reversed flow for q=99 kW/m^2, G=205 kg/(m^2•s), P=0.141 MPa, and ΔT_{in}=15℃.

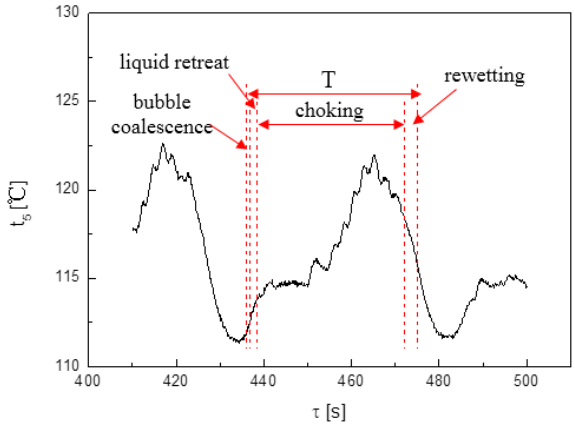

(a) Outer wall temperature.

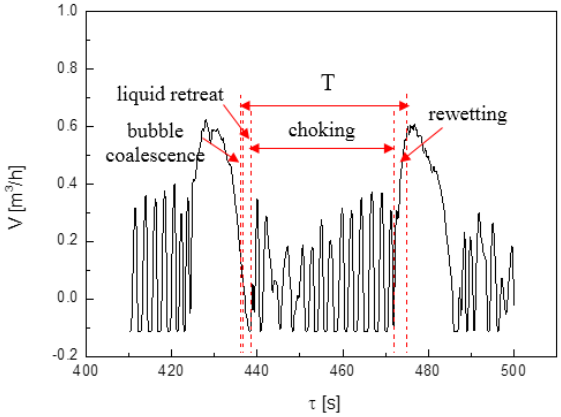

(b) Volume flow rate.

Fig.7 Parameters' fluctuation during one reversed flow period, q=99 kW/m^2, G=205 kg/(m^2•s), P=0.141 MPa, and ΔT_{in}=15℃.

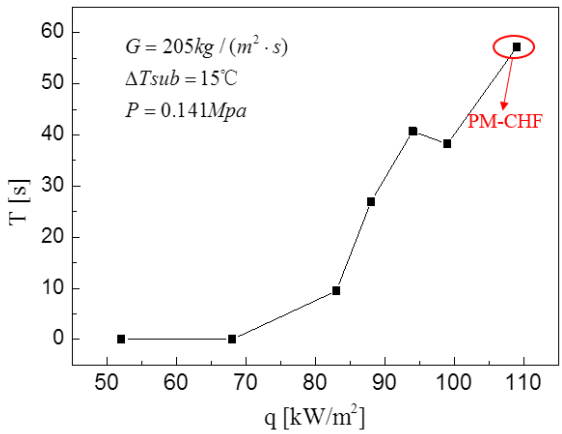

Fig.8 The period of reversed flow with heating flux.

3.2 Fluctuation of parameters

Lee [6] assumed that when the wall temperature exceeded 200 ℃, it could be identified as the PM-CHF. In the present study, PM-CHF was recognized as the maximum heat flux before the outer wall temperature exceeded 200 ℃. Experiments were conducted under different thermal hydraulic conditions including inlet water subcooling and mass flux and the overall results are shown as Table 2. PM-CHF increased with the increasing inlet subcooling and mass flux.

Table. 2 PM-CHF attained in the present experiment under different subcooling and mass flux

Inlet water subcooling (℃)	Mass flux [kg/(m² s)]	PM-CHF (kW/m²)
15	205	83
15	110~123	57
20	110~123	60
20	337	153
34	110~123	81

Fig.9 to Fig.11shows the trend of volume flow rate, pressure drop and outer wall temperature of heating plate during elevating heat flux to PM-CHF. In the process of continuously increasing heating flux, pressure drop, flow rate and outer wall temperature started successively to fluctuate. At 36.36 **kW/m²**, the pressure drop took the lead to fluctuate with distinguishable amplitude. This point could be recognized as the onset of pressure drop fluctuation (OPDF), which marked the onset of flow instability (OFI). With further increase of heat flux, the flow rate followed to fluctuate too. The flowmeter's range was set to be -0.1~0.9 **m³/h**, so the flow rate less than -0.1 **m³/h** could not be measured and was recorded to be -0.1 **m³/h**. The outer wall temperature was the last to fluctuate.

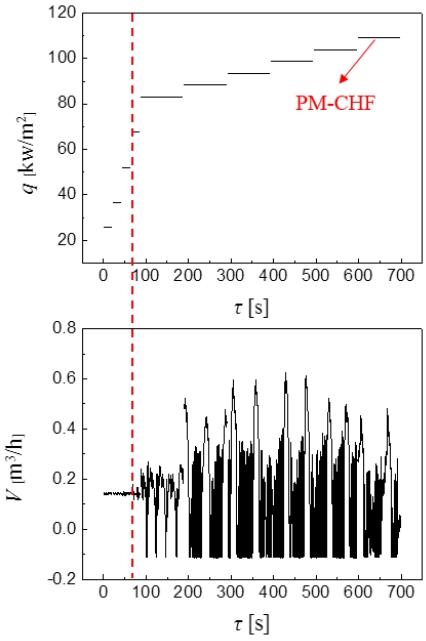

Fig.9 Trend of volume flow rate during elevating heat flux to PM-CHF (ΔT_{sub}=15 ℃, G=205 kg•m^{-2}•s^{-1} , P=0.141 MPa).

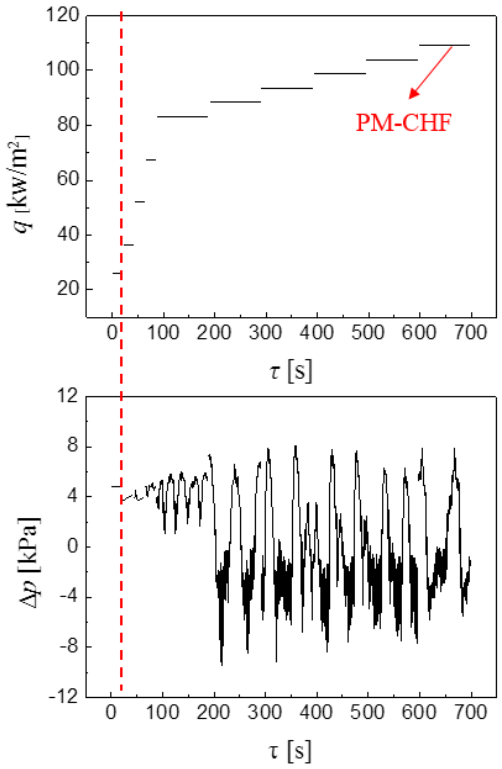

Fig.10 Trend of pressure drop during elevating heat flux to PM-CHF (ΔT_{sub}=15 ℃, G=205 kg•m^{-2}•s^{-1} , P=0.141 MPa).

At the heat flux of 88.31 **kW/m²**, the outer wall temperature started to fluctuate with a significant amplitude and instantaneous temperature once reached 150 ℃. But soon after, the outer wall temperature dropped to 115 ℃ again and fluctuated

with a small amplitude. Finally, as the heat flux reached 109 **kW/m²**, the outer wall temperature increased rapidly to exceed 200 **℃**.

From the above analysis we can see that before the occurrence there would be fluctuation of flow rate and pressure drop, which could be used to prevent the PM-CHF. Pressure drop fluctuation was earlier than that of flow rate. Under the premise of taking into account safety and economy, flow rate fluctuation was chose to prevent the occurrence of PM-CHF.

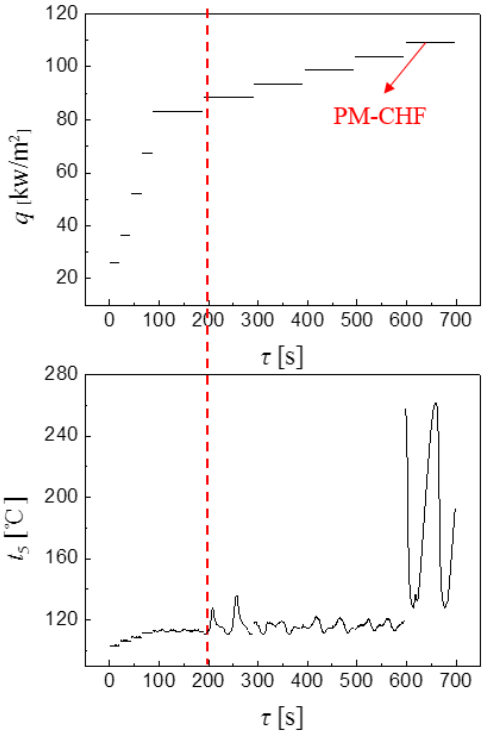

Fig.11 Trend of t_5 during elevating heat flux to CHF (ΔT_{sub}=15 ℃, G=205 kg•m^{-2}•s^{-1} , P=0.141 MPa).

Factors related to system stability are so much that we could not use just two factor to draw a stability region map. Therefore, N_{sub} (dimensionless inlet subcooling number) and N_{pch}[9] (dimensionless phase change number) were chose to depict the stability region map. N_{sub} and N_{pch} could be expressed as follows:

$$N_{sub} = \frac{h_f - h_i}{h_{fg}} \times \frac{\upsilon_{fg}}{\upsilon_f} \quad (1)$$

$$N_{pch} = \frac{Q}{M \times h_{fg}} \times \frac{\upsilon_{fg}}{\upsilon_f} \quad (2)$$

where h_f, h_i, h_{fg}, υ_{fg}, υ_f, Q, and M represents enthalpy of saturated water, inlet enthalpy, latent heat of vaporization, specific volume of saturated vapor, specific volume of saturated water, heating power and mass flow rate, respectively.

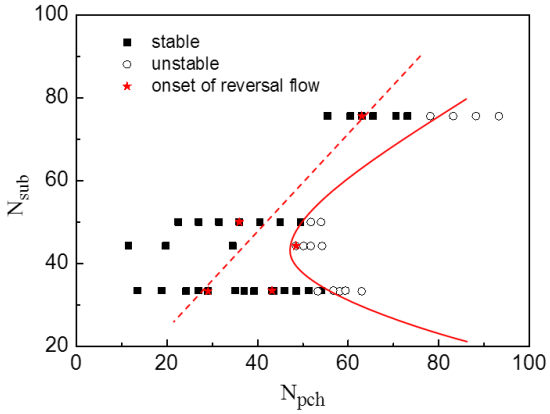

Fig.12 Flow stability region.

Fig.12 is the flow stability region, in which black solid square represents non-CHF condition, hollow circle represents CHF condition, red star represents the onset of reversed flow and the point on the right side of red star represents the condition under which reversed flow happened. As the Fig.12 shows, the non-CHF region is separated from the PM-CHF region by a parabola. At medium N_{sub} (approximately 44), it is the easiest for PM-CHF to happen. When the N_{sub} becomes relatively larger or smaller, larger N_{pch} is needed to induce PM-CHF. The red dotted line is fitted by the points of onset of reversed flow. The lower right area of the line represents the region where reversed flow more easily happens and so does the PM-CHF. Therefore, as long as the operating conditions is in the higher left of the red dotted line, the flow is stable hence the PM-CHF will be avoided.

4. Conclusions

1 The visualization results showed that the reversed flow could be divided into three stages: bubble coalescence, liquid retreat and rewetting. As the heat flux increased sufficiently, a new stage named after choking was observed between the liquid retreat and the rewetting. It was determined that the PM-CHF was induced by the longer and longer reversed flow cycle with the increasing heat flux.

2 Before the occurrence of PM-CHF there would be successive fluctuation of flow rate and pressure drop over the test section. The fluctuation of flow rate can be used as the method to prevent the occurrence of

the PM-CHF. A boundary map to prevent PM-CHF was depicted in terms of dimensionless inlet subcooling number and dimensionless phase change number based on the present experimental configuration. A line representing the boundary between the reversed flow and the stable flow was fitted. The lower right area of the line represented the region where reversed flow more easily happened and so did the PM-CHF. Therefore, as long as the operating conditions is in the higher left of the red dotted line, the flow is stable hence the PM-CHF will be avoided.

Nomenclature

G	mass flux, kg/(m^2 • s)
h	enthalpy, kJ/kg
P	pressure, MPa
q	heat flux
Q	heating power, W
t	temperature, ℃
T	period, s
V	volume flow rate, m^3/h
w	channel width, m
x	quality

Greek symbol

υ	specific volume, m^3/kg
ρ	density, m^3/kg
σ	surface tension, N/m

Subscript

c	critical
e	equilibrium
f	saturated liquid
fg	saturated vapor
in	inlet
pch	phase change
sub	subcooling
w	wall

Acknowledgement

This paper is supported by Nuclear Safety and Simulation Technology Key Laboratory of National Defense Disciplines, Harbin Engineering University, the National Natural Science Foundation of China (No.11605033), National Youth Fund (No.11605032) and the Pre-study of Equipment Department of China National Nuclear Corporation.

References

[1] BERGLES, A. E., and KANDLIKAR, S. G.: On the Nature of Critical Heat Flux in Microchannels[J]. Journal of Heat Transfer, 2005, 127(1):701-707.

[2] QU, W., and MUDAWAR, I.: Measurement and correlation of critical heat flux in two-phase micro-channel heat sinks[J]. International Journal of Heat & Mass Transfer, 2004, 47(10): 2045-2059.

[3] QU, W., and MUDAWAR, I.: Measurement and prediction of pressure drop in two-phase micro-channel heat sinks[J]. International Journal of Heat and Mass Transfer, 2003, 46(15):2737-2753.

[4] KANDLIKAR, S. G., TIAN, S., and STEINKE, M. E., *et al.*: high-speed photographic observation of flow boiling of water in parallel mini-channels[C]// 2001.

[5] LEE, J., and MUDAWAR, I.: Critical heat flux for subcooled flow boiling in micro-channel heat sinks[J]. International Journal of Heat & Mass Transfer, 2009, 52(13):3341-3352.

[6] KIM, S. M., and MUDAWAR, I.: Review of two-phase critical flow models and investigation of the relationship between choking, premature CHF, and CHF in micro-channel heat sinks[J]. International Journal of Heat & Mass Transfer, 2015, 87:497-511.

[7] LEE, J., JO, D., and CHAE, H., *et al.*: The characteristics of premature and stable critical heat flux for downward flow boiling at low pressure in a narrow rectangular channel[J]. Experimental Thermal & Fluid Science, 2015, 69:86-98.

[8] KAYA, A., ÖZDEMIR, M. R., and KESKINÖZ, M., *et al.*: The effects of inlet restriction and tube size on boiling instabilities and detection of resulting premature critical heat flux in microtubes using data analysis[J]. Applied Thermal Engineering, 2014, 65(1-2):575-587.

[9] RUSPINI, L. C., MARCEL, C. P., and CLAUSSE, A.: Two-phase flow instabilities: A review[J]. International Journal of Heat and Mass Transfer. 71(2014): 521-548.